# Image processing with nonseparable multiwavelets

Ana M. C. Ruedin
Departamento de Computación
Facultad de Ciencias Exactas y Naturales
Universidad de Buenos Aires
E-mail: anita@dc.uba.ar

December 22, 2000

**Abstract**

In a general context we introduce image processing with 1-dimensional wavelets and show the differences with nonseparable 2-dimensional wavelets having quincunx decimation, in the first place, and with balanced nonseparable 2-dimensional multiwavelets, in the second place. All of them are orthogonal. Formulae for analysis and synthesis are given for the latter. The first steps are illustrated with images. The decomposition of the original image into 2 input images is explained. We illustrate with examples 2 applications: zoom-in (interpolation) and compression of images.

Keywords: multiwavelets, nonseparable, quincunx.

## 1 INTRODUCTION

Wavelet transforms have good time-frequency localization, which makes them an efficient tool for signal processing: they are used for compression, denoising, zooming an image. Generalizations of wavelets include i) nonseparable wavelets and ii) multiwavelets. We show how a combination of both works in practice, and give examples of two applications.

In section 2 we briefly introduce image processing with 1-dimensional wavelets. In section 3 we show how these are used to process images –the separable wavelets– and how a more general approach includes 2-d filters and decimation with a dilation matrix. We illustrate this defining quincunx decimation.

In section 4 multiwavelets are introduced, and in section 5 nonseparable multiwavelets are introduced. Formulae for analysis and synthesis are given for the latter in section 6. The first steps are illustrated with images. The decomposition of the original image into 2 input images is explained. Finally we illustrate with examples two applications: zoom-in (interpolation) and compression of images

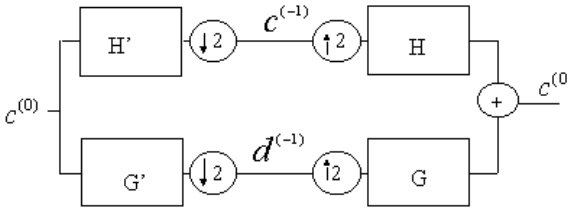


Figure 1: Analysis-synthesis scheme

## 2 Wavelet processing a 1-d signal

Given a one-dimensional signal $c_k^{(0)}$, finding one step of the wavelet transform of the signal consists in i) filtering the signal with a low-pass filter $H' = [..h_3\ h_2\ h_1\ h_0..]$ and carrying out a decimation by 2, giving a smoothed version of the signal $c_k^{(-1)}$ ( approximation coefficients ), and ii) filtering the signal with a high-pass filter $G'$and carrying out a decimation by 2, giving the detail coefficients $d_k^{(-1)}$, which capture the fine details of the signal. In figure 1 we have the transform and inverse transform scheme. Two functions define the wavelet transform: the scaling function $\Phi(x)$ and the wavelet $\Psi(x)$, which verify:

$$\Phi(x) = \sum_{k \in \Lambda \subset Z} h_k \quad \Phi(\ 2\ x - k\ \ ) \qquad\qquad \Psi(x) = \sum_{k \in \Lambda \subset Z} g_k \quad \Phi(\ 2\ x - k\ \ )$$

Coefficients $c_k^{(0)}$ correpond to a certain function $f(x)$ written in the basis of integer translations of the scaling function: $\{\Phi(\ x - k)\}$, and under certain conditions the $\{c_k^{(0)}\}$ are very close to the samples of $f(x)$ (see [Daubechies1992]).

$$f(x) = \sum_k c_k^{(0)} \Phi(x - k)$$

Coefficients $c_k^{(-1)}$ correpond to the basis $\{\frac{1}{\sqrt{2}}\ \Phi(\ \frac{x}{2} - k)\}$ and $d_k^{(-1)}$ correpond to the basis $\{\frac{1}{\sqrt{2}}\ \Psi(\ \frac{x}{2} - k)\}$

In a second step the whole process is repeated on $c_k^{(-1)}$: we now obtain the coarser approximation coefficients $c_k^{(-2)}$, and the detail coefficients $d_k^{(-2)}$, which correspond to less fine detail. We end up having a very coarse approximation of the original signal, and a series of details at different scales.

$$f(x) = \sum_k c_k^{(-L)} \Phi_{-L,k}(x) + \sum_{j=-L+1}^{-1} \sum_k d_k^{(j)} \Psi_{j,k}(x) \qquad (1)$$

where

$$\Phi_{j,k}(x) = 2^{j/2}\ \ \Phi(2^j\ \ x - k)\ \ ; \Psi_{j,k}(x) = 2^{j/2}\ \ \Psi(2^j\ \ x - k)$$

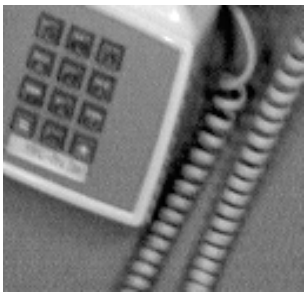

Figure 2: Original image

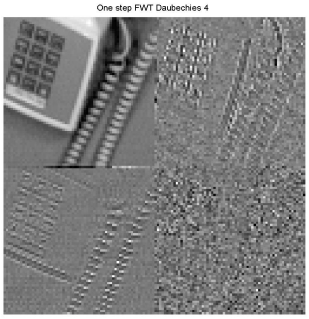


Figure 3: One step of the separable Daubechies 4 transform

Scaling functions and wavelets can be constructed to have certain useful properties such as short support, orthogonality, symmetry, and polynomial approximation. However, except for the Haar wavelet there can be no symmetry and orthogonality simultaneously for real filters.

# 3 Wavelets for image processing

The way to process an image with 1d- wavelets is to apply the transform to the rows and then to the columns of the resulting image. In figure 2 we have the original image of a phone, and and in figure 3 we have one step of the separable Daubechies 4 transform. At the upper left corner is the phone at a coarser resolution; the 3 other submatrices correspond to details, which are mostly oriented in the vertical and horizontal directions. However, this does not agree with our visual perception.

To avoid this, images are treated with nonseparable filters, and the decimation is done with a general dilation matrix. Examples of nonseparable bidimensional wavelets have been given.( [Cohen and Daubechies1993],

[Kovacevic and Vetterli1992], and [Kovacevic and Vetterli]).

### 3.1 Nonseparable wavelets :Quincunx (diagonal) decimation and upsampling

We consider two possible dilation matrices: $D_1$, a reflection followed by an expansion of $\sqrt{2}$, and $D_2$, a rotation followed by an expansion of $\sqrt{2}$. For both matrices $|D| = |\det(D)| = 2$.

$$D_1 = \begin{bmatrix} 1 & 1 \\ 1 & -1 \end{bmatrix} \qquad D_2 = \begin{bmatrix} 1 & -1 \\ 1 & 1 \end{bmatrix}$$

Both $D_1$ and $D_2$ induce a decomposition of the sets of all pairs of integers $Z^2$ into 2 cosets: $\Gamma_1$ and $\Gamma_2$, forming the quincunx sublattices -black and white squares of a chess-table:

$$Z^2 = \Gamma_1 \cup \Gamma_2 \;\; ; \;\; \Gamma_1 = \{DZ^2\} \;\; ; \;\; \Gamma_2 = \left\{ DZ^2 + \begin{bmatrix} 1 \\ 0 \end{bmatrix} \right\}$$

Let $D$ be the dilation matrix.
We define decimation of an image with $D$ as
$Y = X \downarrow D \iff Y_k = X_{Dk}$.
We define upsampling an image with $D$ as:
$Y = X \uparrow D \Leftrightarrow Y_k = \begin{cases} X_j, & if\ k = Dj\ for\ some\ j \in Z^2 \\ 0 & if\ D^{-1}k \notin Z^2 \end{cases}$

For example, if we have image $X = \begin{bmatrix} 1 & 2 \\ 3 & 4 \end{bmatrix}$, then $X$ upsampled with $D_1$ is $Y = \begin{bmatrix} 0 & 1 & 0 \\ 2 & 0 & 3 \\ 0 & 4 & 0 \end{bmatrix}$. The dilation matrix is a reflection, and it induces a reflection in the upsampled image $Y$. If $Y$ is now decimated with $D_1$, we recover $X$. Quincunx decimation is equivalent to eliminating all the white squares of a chess-table.

## 4 Multiwavelets

In a more general context, we consider the approximation images as generated by the integer translations of 2 or more scaling functions: they give rise to multi-scaling functions and multiwavelets. Multiwavelets in 1-d have been constructed to have suitable properties, such as orthogonality, polynomial approximation, short support and symmetry. They have given good results for signal compression: see [Strela1996] [Strela *et al.*to appear] and [Plonka and Strela1998]. Balanced multiwavelets [Lebrun and Vetterli1997] were introduced in order to avoid prefiltering the input data, so that the lowpass branch of the transform preserves discretized polynomials.

# 5 Nonseparable multiwavelets.

In previous works [Ruedin1999] [Ruedin2000] the author constructed examples of continuous balanced nonseparable orthogonal multiscaling functions, in an attempt to combine advances made in both directions: multiwavelets, and nonseparable bidimensional wavelets. They are compactly supported, have quincunx decimation, and have polynomial approximation orders (i.e. accuracy) 2 and 3. Their corresponding multiwavelets were also found. (To obtain the filter coefficients please e-mail the author.) We give a short outline of the theory.

Let $\Phi_1$ and $\Phi_2$ be 2 continuous scaling functions defined over $R^2$ and associated to a dilation matrix $D$. In vector form the dilation equation becomes

$$\Phi(x) = \sum_{k \in \Lambda \subset Z^2} H_k \;\; \Phi(\; D\; x - k \;\;)$$

$$\left[ \begin{array}{c} \Phi_1(x) \\ \Phi_2(x) \end{array} \right] = \sum_k [H_k \;\;] \left[ \begin{array}{c} \Phi_1(\;\; D\; x - k \;) \\ \Phi_2(\;\; D \;\; x - k \;) \end{array} \right] \tag{2}$$

where $H_k$ are 2x2 matrices with indices

$$M_{0=} \left[ \begin{array}{cccc} 0 & H_{1,1} & H_{2,1} & 0 \\ H_{0,0} & H_{1,0} & H_{2,0} & H_{3,0} \\ 0 & H_{1,-1} & H_{2,-1} & 0 \end{array} \right]$$

and $D$ is the dilation matrix. Notation is rather loose and $\Phi_1(\; D\; x - k\;)$ means that we apply $\Phi_1$ to the 2 entries of $D\; x - k = \left[ \begin{array}{cc} d_{11} & d_{12} \\ d_{21} & d_{22} \end{array} \right] \left[ \begin{array}{c} x_1 \\ x_2 \end{array} \right] - \left[ \begin{array}{c} k_1 \\ k_2 \end{array} \right]$

The number of wavelets is $|D| - 1 = 1$ in both cases. The equation for the multiwavelet, in vector form, is:

$$\Psi(x) = \sum_k G_k \;\; \Phi(\; D\; x - k\;) \tag{3}$$

# 6 Analysis-synthesis formulae:

Assume that we decompose the original image into two input images $c^{(0)}_{1,k}$ and $c^{(0)}_{2,k}$ $(k \in Z^2)$, and let $f(x)$ be the function that verifies:

$$f(x) = \sum_{k \in Z^2} c^{(0)T}_{\cdot,k} \Phi(x - k), \quad \text{where } c^{(0)}_{\cdot,k} = \left[ \begin{array}{c} c^{(0)}_{1,k} \\ c^{(0)}_{2,k} \end{array} \right].$$

The analysis scheme (see figure 6) outputs 2 approximation images: $c^{(-1)}_{1,k}$ and

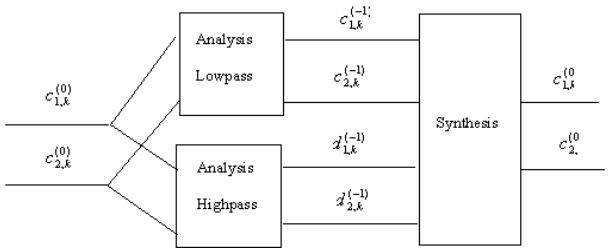


Figure 4: Analysis-synthesis scheme

$c_{2,k}^{(-1)}$, and 2 detail images: $d_{1,k}^{(-1)}$ and $d_{2,k}^{(-1)}$,whose expression we want to find. We set

$$c_{\cdot,k}^{(-1)} = \begin{bmatrix} c_{1,k}^{(-1)} \\ c_{2,k}^{(-1)} \end{bmatrix} \qquad d_{\cdot,k}^{(-1)} = \begin{bmatrix} d_{1,k}^{(-1)} \\ d_{2,k}^{(-1)} \end{bmatrix}.$$

$$c_{\cdot,k}^{(-1)} = \frac{1}{\sqrt{|D|}} \sum_{j \in Z^2} H_{j-Dk}\ c_{\cdot,j}^{(0)} \tag{4}$$

$$d_{\cdot,k}^{(-1)} = \frac{1}{\sqrt{|D|}} \sum_{j \in Z^2} G_{j-Dk}\ c_{\cdot,j}^{(0)}. \tag{5}$$

Similarly it can be shown that the *synthesis formula* is:

$$c_{\cdot,k}^{(0)} = \frac{1}{\sqrt{|D|}} \left[ \sum_{j \in Z^2} H_{k-Dj}^T c_{\cdot,j}^{(-1)} + \sum_{j \in Z^2} G_{k-Dj}^T d_{\cdot,j}^{(-1)} \right] \tag{6}$$

In figure 5 we have 4 images: they are the coefficients of one step of the multiwavelet transform: $d_{1,k}^{(-1)}$ (top left), $c_{1,k}^{(-1)}$ (top right) and $d_{2,k}^{(-1)}$ (bottom left), $c_{2,k}^{(-1)}$ (bottom right). The dilation matrix was $D_1$ The effect of downsampling with $D_1$ in the analysis formula is to reflect and contract the image.

In figure 6 are the coefficients of 2 steps of the same transform: $d_{1,k}^{(-1)}$, $d_{1,k}^{(-2)}$, $c_{1,k}^{(-2)}$ (top) and $d_{2,k}^{(-1)}$, $d_{2,k}^{(-2)}$ , $c_{2,k}^{(-2)}$ (bottom). After 2 steps the image has recovered its original orientation. It takes 4 steps to do so if the dilation matrix is $D_2$.

At each step, before the images are processed they have to be periodized, otherwise there are artifacts at the borders. Periodization is different if the frames of the images are normally oriented squares (after the even steps) or diamond-oriented squares (after the odd steps).

At the beginning of the process the original image may be copied so as to get 2 input images. Otherwise, the original image can be decomposed into 2 input images by separating into 2 diamonds the pixels belonging to each coset

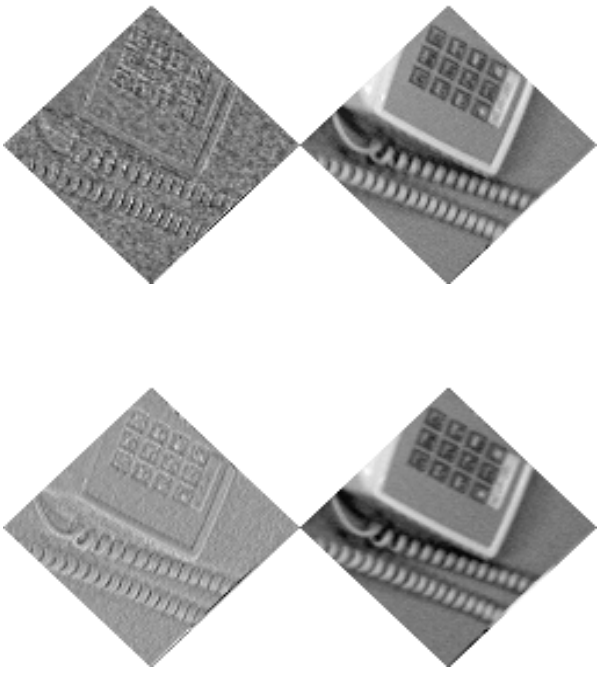

Figure 5: One step of the multiwavelet transform

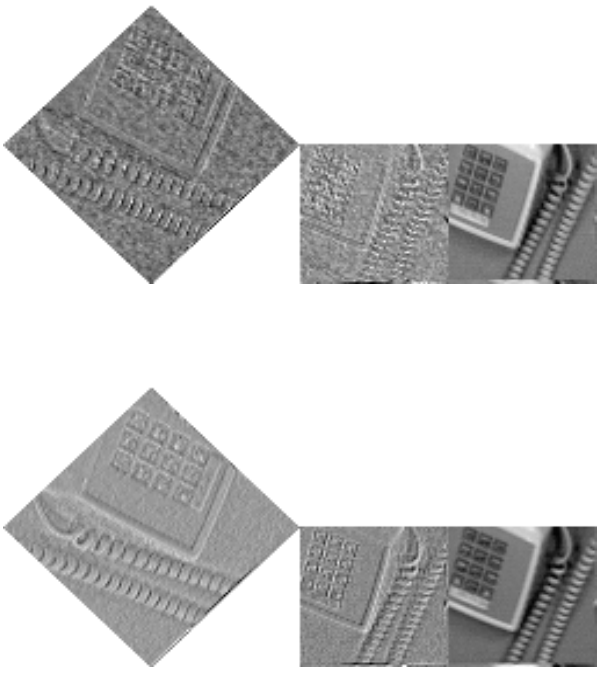

Figure 6: 2 steps of the multiwavelet transform

Figure 7: Zoom-in with Daubechies 4

Figure 8: Zoom-in with D1-acc3-bal

Notice that in this way all the coefficients of the multiwavelet transform need as much storage as the original image, and can be made to fit into it.

# 7 Applications:

## 7.1 Zoom in

To zoom-in an image with one-dimensional wavelets, we upsample the image and then convolve it with a low-pass filter – i.e we apply the synthesis algorithm of scheme 1 to the image, after setting to zero the detail coefficients.

To zoom-in an image with nonseparable multiwavelets, we apply the synthesis algorithm of scheme 6: the image is copied onto $c_{1,\cdot}^{(-1)}$ and $c_{2,\cdot}^{(-1)}$, the details $d_{1,\cdot}^{(-1)}$ and $d_{2,\cdot}^{(-1)}$ are set to zero and the synthesis formula 6 is applied.

The original image of a phone was decimated eliminating 3 pixels out of 4. It was then zoomed-in with separable Daubechies 4 wavelet, on one hand (see detail in figure 7.1), and with a nonseparable balanced multiwavelet having accuracy 3 with dilation matrix $D_1$ –$D1-acc3-bal$ –, on the other (see detail in figure 7.1). Comparing both images, we see that the latter has more resolution; this is because the dilation matrix takes 2 steps to zoom-in an image to twice its size; while with separable wavelets it takes 1 step.

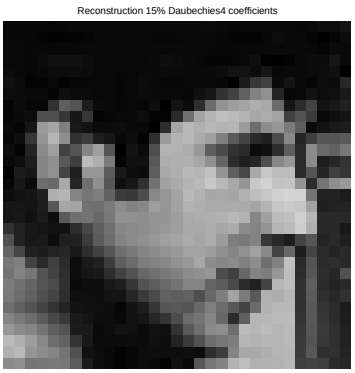


Figure 9: Reconstruction with Daubechies 4 -detail

### 7.2 Compression

Wavelet transforms are efficient for image compression: they decorrelate the data and give a sparse representation of the image. A threshold is applied to the transformed coefficients; the thresholded coefficients have many zeroes and this is useful for compression. The quality of the reconstructed image is good. Since the system is orthonormal, an error in the transformed coefficients is equal to the error in the reconstructed image (in 2-norm).

The original image of a cameraman was chosen for compression. The separable wavelet transform Daubechies 4 and the multiwavelet transform $D1 - acc3 - bal$ were applied to it and compared. The number of steps taken was such that the final coarse approximation matrix was of size $8 \times 8$. The original images were compressed retaining in all cases 15% of the largest transformed coefficients in absolute value –adecuate quantization and entropy coding will improve the compression rate. In figure 9 we have a detail of the reconstructed image after transforming with Daubechies 4 and thresholding. In figure 10 we have a detail of the reconstructed image after transforming with $D1 - acc3 - bal$ multiwavelet and thresholding. The latter looks smoother, but the former has more energy compaction: the PSNR was 35.51 for Daubechies 4 and 32.20 for $D1 - acc3 - bal$.

## 8 Conclusion

We have shown how image processing is achieved with nonseparable multiwavelets having quincunx decimation. The examples reveal satisfactory results at interpolation ( zoom- in) for these wavelets. For future work remains the construction of better filters for image compression.


Figure 10: Reconstruction with $D1 - acc3 - bal$ –detail

# References

[Cohen and Daubechies1993] A. Cohen and I. Daubechies. Non-separable bidimensional wavelet bases. *Revista Matematica Iberoamericana*, 9:51–137, 1993.

[Daubechies1992] I. Daubechies. *Ten lectures on wavelets*. Society for Industrial and Appl Mathematics, 1992.

[Kovacevic and Vetterli] J. Kovacevic and M. Vetterli. New results on multidimensional filter banks and wavelets. *preprint*.

[Kovacevic and Vetterli1992] J. Kovacevic and M. Vetterli. Nonseparable multidimensional perfect reconstruction filter banks and wavelet bases for $r^n$. *IEEE, Transactions on Information Theory*, 38(2):533–555, 1992.

[Lebrun and Vetterli1997] J. Lebrun and M. Vetterli. Balanced multiwavelets: Theory and design. *IEEE Transactions on Signal Processing*, 1997.

[Plonka and Strela1998] G. Plonka and V. Strela. Construction of multiscaling functions with approximation and symmetry. *SIAM Journal of Mathematical Analysis*, 29:481–510, 1998.

[Ruedin1999] A. Ruedin. Nonseparable orthogonal multiwavelets with 2 and 3 vanishing moments on the quincunx grid. *Proceedings SPIE Wavelet Appl. Signal Image Proc. VII*, 3813:455–466, 1999.

[Ruedin2000] A. Ruedin. Balanced nonseparable orthogonal multiwavelets with 2 and 3 vanishing moments on the quincunx grid. *Proceedings SPIE Wavelet Appl. Signal Image Proc. VIII*, 4119:to appear, 2000.

[Strela *et al.*to appear] V. Strela, P. Heller, G. Strang, P. Topiwala, and C. Heil. The application of multiwavelet filter banks to signal and image processing. *IEEE Transactions in Image Processing*, to appear.

[Strela1996] V. Strela. *Multiwavelets: Theory and Applications.* PhD thesis, 1996.